CLIMATE CHANGE

10.1126/sciadv.1500560

Future extreme sea level seesaws in the tropical Pacific

Matthew J. Widlansky,[1]* Axel Timmermann,[1,2] Wenju Cai[3]

Global mean sea levels are projected to gradually rise in response to greenhouse warming. However, on shorter time scales, modes of natural climate variability in the Pacific, such as the El Niño–Southern Oscillation (ENSO), can affect regional sea level variability and extremes, with considerable impacts on coastal ecosystems and island nations. How these shorter-term sea level fluctuations will change in association with a projected increase in extreme El Niño and its atmospheric variability remains unknown. Using present-generation coupled climate models forced with increasing greenhouse gas concentrations and subtracting the effect of global mean sea level rise, we find that climate change will enhance El Niño–related sea level extremes, especially in the tropical southwestern Pacific, where very low sea level events, locally known as *Taimasa*, are projected to double in occurrence. Additionally, and throughout the tropical Pacific, prolonged interannual sea level inundations are also found to become more likely with greenhouse warming and increased frequency of extreme La Niña events, thus exacerbating the coastal impacts of the projected global mean sea level rise.

INTRODUCTION

The largest interannual variability of sea level occurs in the tropical Pacific (Figs. 1 and 2A) and is a well-known aspect of El Niño–Southern Oscillation (ENSO) (*1*–*3*) and its interaction with the annual cycle (*4*–*8*). During strong El Niño events, such as observed in 1982–1983 and 1997–1998, sea level drops around tropical western Pacific islands by up to 20 to 30 cm (Fig. 1) (*9*). Such extreme low sea levels expose shallow reefs (referred to in Samoa as "*Taimasa*," which means foul-smelling tide) (*8*, *10*), thereby damaging associated coastal ecosystems and contributing to the formation of "flat-topped coral heads" often referred to as microatolls (*11*). At the same time, sea levels rise in the eastern Pacific—especially along the equator, where anomalies exceeding 35 cm have been recorded around the Galápagos Islands (*12*)—stressing coastal ecosystems by sea level high stands (*13*). This Pacific-wide sea level seesaw generally reverses during La Niña, although the anomalies rarely exceed 10 cm (Fig. 1) and coastal impacts are typically less severe (*14*).

Such sea level extremes are caused by wind-driven, massive zonal and meridional shifts of the tropical Pacific thermocline, associated with ENSO (*1*, *15*). During El Niño, weak equatorial trade winds cause the thermocline to shoal in the tropical western Pacific and deepen to the east, producing a zonal sea level pattern that mirrors these subsurface changes (*16*). Meridional asymmetry in sea level is most pronounced during strong El Niño events (*17*), such as in 1982–1983 and 1997–1998. The meridional sea level pattern has recently been linked to near-equatorial collapses of the South Pacific Convergence Zone (SPCZ) (*8*). These so-called zonal SPCZ events (*18*)—and the associated wind stress anomalies (*19*, *20*) that force oceanic Ekman suction (*21*) and cause sea level drops (*22*)—prolong the negative effects of *Taimasa* throughout the equatorial central and tropical southwestern Pacific.

Recent modeling studies project an increase in the number of zonal SPCZ events (*18*), as well as extreme El Niño (*23*) and La Niña (*24*) events, in response to greenhouse warming. How these projections translate into changes in interannual sea level extremes in the tropical Pacific has not been examined (*25*). Using a set of global climate models that capture the main observed modes of interannual wind and sea level variability, we here show that there is an increase in future extreme sea level events with greenhouse warming.

RESULTS

State-of-the-art coupled general circulation models (CGCMs) simulate the salient features of interannual sea level variability in the tropical Pacific reasonably well (*26*), although model performance varies considerably and some simulations suffer large global sea level drifts (fig. S1), which we remove for our analysis. Examining simulations conducted as part of the Coupled Model Intercomparison Project phase 5 (CMIP5) (table S1) (*27*), which can simulate the observed nonlinear relationship between the leading modes of precipitation (*18*) and wind variability in the Pacific (see Materials and Methods for model selection criteria), one finds that the future interannual variability of sea level is expected to increase by 2100 in almost the entire tropical Pacific for the representative concentration pathway 8.5 (RCP8.5) (Fig. 2B; 5 to 25% change in SD). The changes are most pronounced in the region centered around the date line in the equatorial Pacific, where the observed sea level variability, represented here by the European Centre for Medium Range Weather Forecasts operational ORA-S4 (*28*), is less than in either the western or the eastern Pacific (Fig. 2A; 4 cm SD compared to up to 10 cm). Past sea level extremes here followed strong El Niño events and are associated with winds accompanying the zonal collapse of the SPCZ (*8*). These future changes are not as pronounced in the CGCMs that fail to simulate the nonlinear characteristics of Pacific rainfall variability (fig. S2).

The variability of the present-day observed annual cycle of sea level in the tropical Pacific (Fig. 2C) is largest in a series of horizontal bands adjacent the mean location of wind stress convergence associated with the Intertropical Convergence Zone (ITCZ) and the SPCZ. The largest

[1]International Pacific Research Center, University of Hawai'i at Mānoa, 1680 East-West Road, Honolulu, HI 96822, USA. [2]Department of Oceanography, University of Hawai'i at Mānoa, 1000 Pope Road, Honolulu, HI 96822, USA. [3]Commonwealth Scientific and Industrial Research Organisation (CSIRO) Oceans and Atmosphere Flagship, 107–121 Station Street, Aspendale, Victoria 3195, Australia.
*Corresponding author. E-mail: mwidlans@hawaii.edu

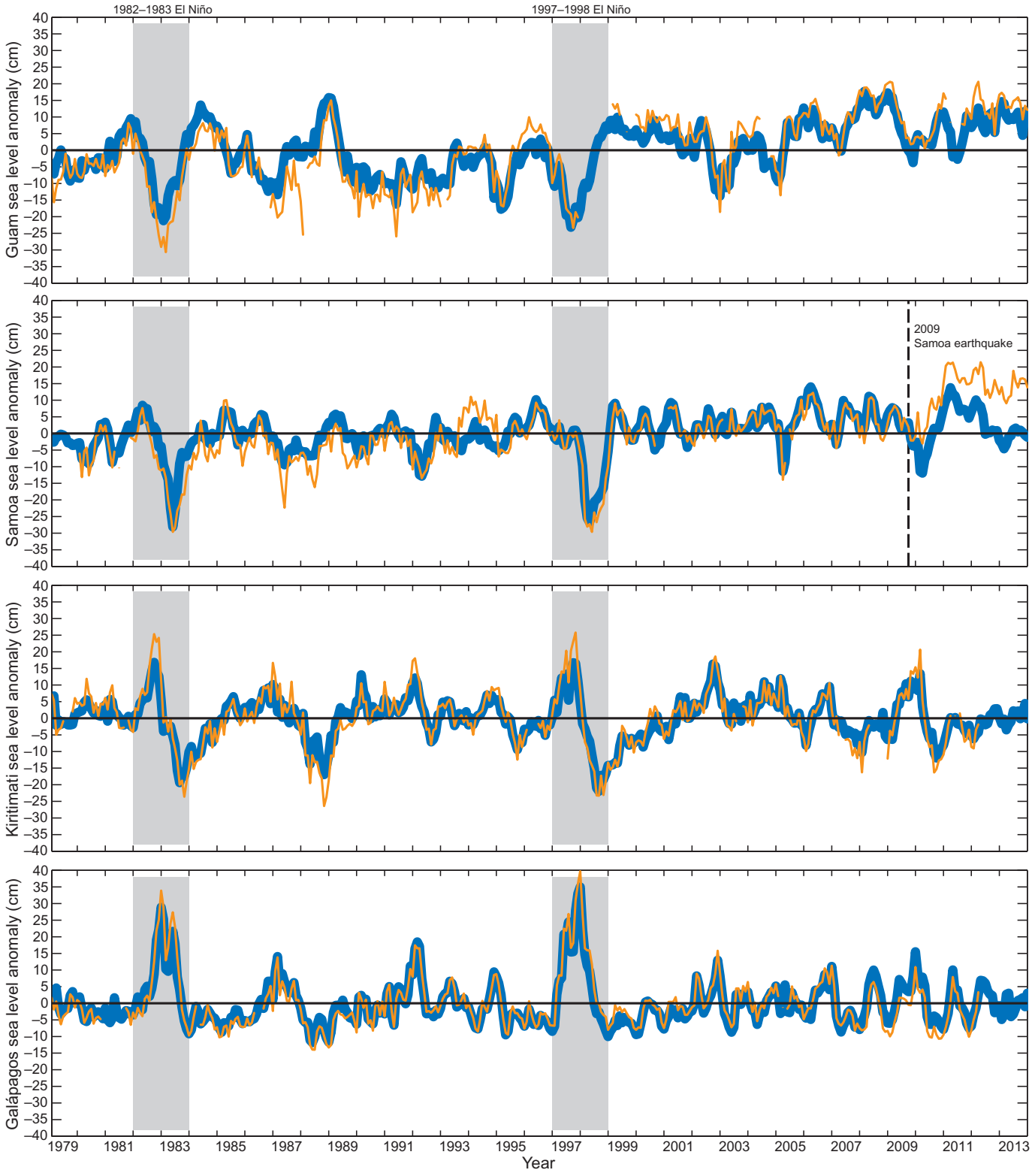

Fig. 1. Observed sea level anomalies (1979–2013; see Materials and Methods) from Ocean Reanalysis System 4 (ORA-S4) (blue) and available tide gauge records (orange) around Guam (Apra Harbor), Samoa (Pago Pago), central Line Islands (Kiritimati), and the Galápagos Islands (Santa Cruz), respectively. Locations are shown in Fig. 2A (4° latitude × 4° longitude averaging regions for ORA-S4). Here, any long-term trends are retained and there is no filtering to remove stochastic noise. The strong El Niño events during 1982–1983 and 1997–1998 are highlighted. There is close correspondence between ORA-S4 and tide gauges, except around Samoa since the 2009 earthquake (dashed line).

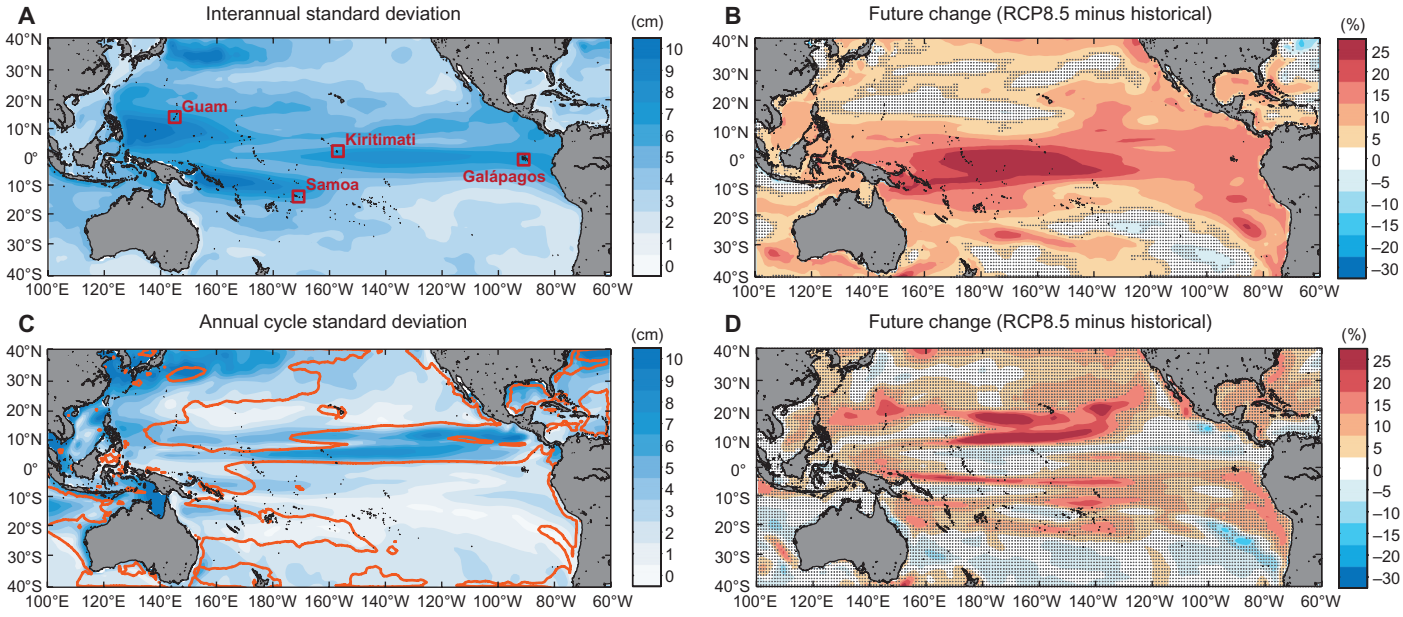

Fig. 2. Observed sea surface height variability on interannual (top) and annual cycle (bottom) time scales and the corresponding CMIP5 21st-century projections. (**A** and **C**) Observed (1979–2013) SD of sea surface height (cm). The red boxes in (A) represent island averaging regions used in Fig. 5. Orange contours in (C) enclose large annual cycle variations in wind stress curl (SD exceeding 3.5×10^{-8} s^{-1}). (**B** and **D**) Multimodel projection (22 models that simulate the observed nonlinear relationship between El Niño and the SPCZ) (*18*) for RCP8.5 (2006–2100) with respect to the historical experiment (1911–2005) for the SD of interannual and annual cycle variability (% change). Stippling denotes regions with no significant change in the multimodel variance according to a two-sample *F* test ($P < 95\%$) with degrees of freedom specified by either the number of model-years (B, 22 models × 95 years) or model-months (D, 22 models × 12 months), respectively, for interannual and annual cycle changes.

projected future greenhouse warming changes of the sea level annual cycle (Fig. 2D) are found adjacent and poleward of the observed maximum annual cycle (Fig. 2C). In contrast, changes along the equator are relatively small and not significantly different from the historical experiment. The future change pattern is consistent with a projected increased annual cycle of the Pacific climate (*29*) that enhances the meridional range of wind stress curl anomalies associated with the margins of the ITCZ (in the Northern Hemisphere) and SPCZ (Southern Hemisphere), which are projected to have more extreme swings with greenhouse warming (*18*, *23*, *24*).

By calculating empirical orthogonal functions (EOFs) of sea surface height anomalies from ORA-S4, we can decompose interannual sea level variability into two leading modes of variability. The spatial patterns of observed EOF1 and EOF2 show the zonal and meridional seesaws of sea surface height anomalies (Fig. 3, insets) previously detected in the tropical Pacific (*8*, *16*, *17*), which are associated with ENSO and the ENSO/annual cycle combination tone (*7*), respectively. As evidenced by the principal component time series of EOF1 and EOF2 (PC1 and PC2), the zonal seesaw (Fig. 3A) peaks during each El Niño, but only two extremes (>3 SDs) of the meridional seesaw (Fig. 3B) have been observed since 1979. Both extremes of the meridional pattern occurred during the termination of the strong El Niños of 1982–1983 and 1997–1998.

Examining sea surface heights from the 20th-century CMIP5 simulations, by projecting the simulated anomalies from each model onto the observed EOF1 and EOF2 patterns (Fig. 3, insets), we find no obvious change in either the occurrence or the amplitude of the zonal or meridional sea level oscillations (Fig. 3, A and B, respectively). In contrast, for the 21st century, the variance of both EOF projections increases compared to that for the 20th century. In the future simulations, the EOF1 and EOF2 time series have a higher number of strong and extreme amplitudes (>±2 and ±3 SDs, respectively), suggesting an increased likelihood of zonal and meridional sea level seesaws in response to greenhouse warming. Along with this increased occurrence of extreme amplitudes, there is a clear trend toward more months with a positive EOF2 projection. We note that the spatial patterns of the simulated zonal and meridional seesaws (fig. S3) resemble the observed patterns (Fig. 3, insets) for both the historical and future periods. These results suggest that below-normal sea levels will become more frequent in the tropical southwestern and equatorial central Pacific, consistent with the likely future doubling of zonal SPCZ events (*18*) and more extreme future wind stress curl anomalies associated with ENSO, the annual cycle, and combinations thereof (fig. S4).

The leading two patterns of sea level variability exhibit an asymmetric, nonlinear relationship (Fig. 4A) between PC1 and the 8-month lagged PC2 (Fig. 4A, inset), which is dominated by extreme values in positive PC1 and PC2 that correspond to the El Niño *Taimasa* events (*8*). Similar extreme values for La Niña events are absent. The fact that extreme amplitudes of the EOF2 projection lag EOF1 prolongs sea level anomalies in those regions of the Pacific where the EOF patterns are of the same sign (see Fig. 3, insets), potentially enhancing local impacts from El Niño such as low sea level stands and coral die-offs. The opposite pattern combination (EOF1 and EOF2 projections <–2 SDs) has never been observed, but such an event—should one ever occur—would be associated with prolonged

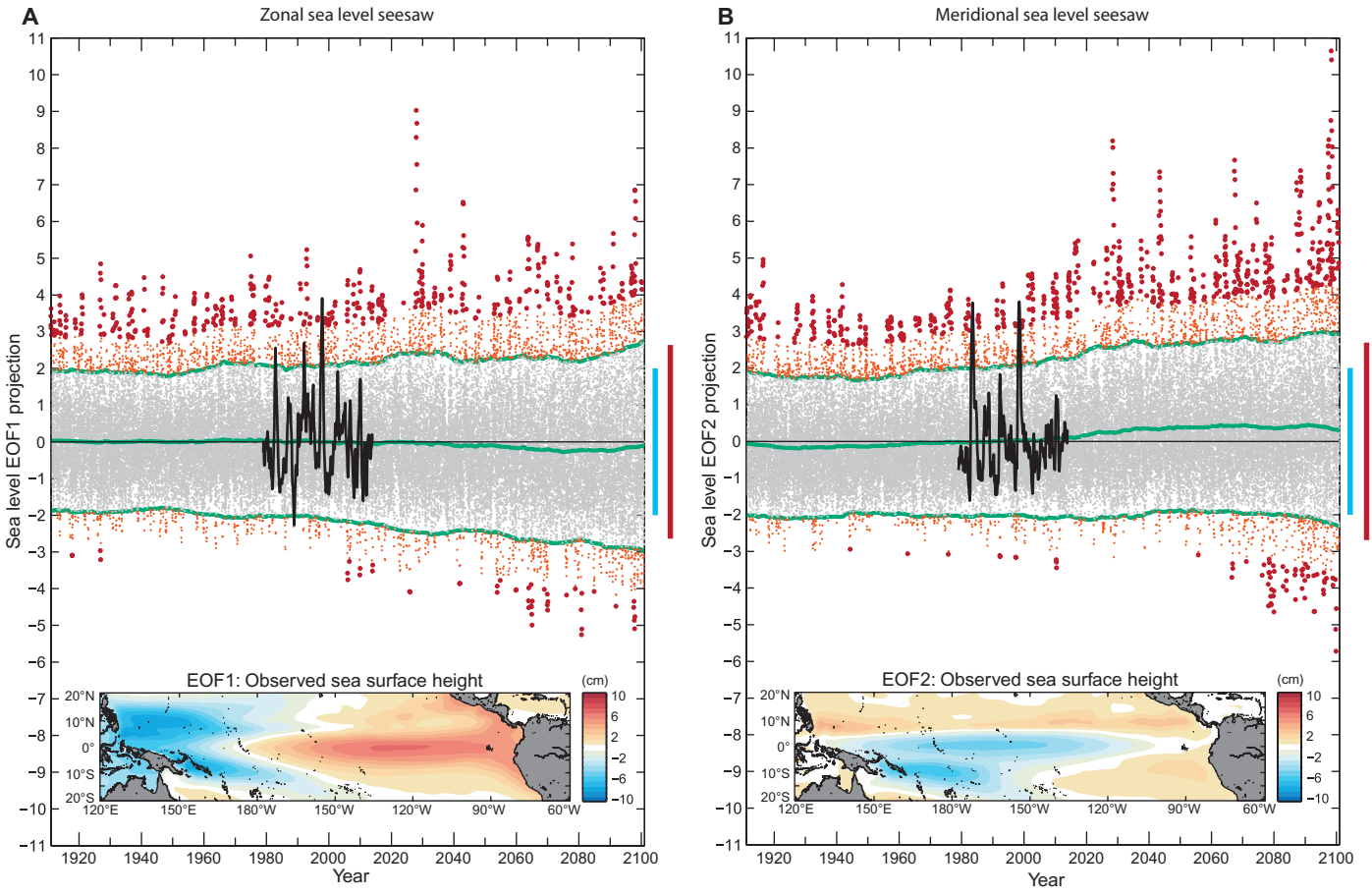

Fig. 3. Two principal modes of sea surface height variability observed (1979–2013; black lines) in the tropical Pacific and the CMIP5-simulated sea surface height anomalies (dots) for the historical (1911–2005) and RCP8.5 (2006–2100) experiments projected onto the observed EOF1 and EOF2 patterns (maps). (**A** and **B**) EOF1 (EOF2) explains 43% (14%) of the observed variance, and the SDs of these modes are projected to increase by 32 and 35%, respectively (RCP8.5 minus historical; blue and red vertical bars indicate the ±2 SD range of the historical and RCP8.5 periods, respectively). Green lines show the 20-year running mean and ±2 SD range of the principal modes. Strong and extreme events are shaded (orange and red, respectively, exceeding the ±2 or ±3 running SD range).

coastal inundations in the same regions affected by *Taimasa*. Such sea level high stands (that is, summing the opposite of the leading patterns of sea level variability shown in Fig. 3, insets) are perceivable should future changes occur in the wind stress curl associated with the orientation of the SPCZ, perhaps influenced by future extreme La Niña events (*24*) combined with changing mean sea surface temperatures (*30*). The nonlinear relationship between the zonal and meridional seesaw modes (Fig. 4A) is also reminiscent of similar characteristics for the rainfall variability in the Pacific (*18*, *23*) and equatorial wind stress (fig. S5).

With greenhouse warming and changing wind stress patterns (figs. S5 and S6), the combined EOF1-EOF2 sea level relationship is projected to become more nonlinear (Fig. 4B). That is, future changes are most pronounced when both sea level modes are of the same sign—either positive or negative—and, furthermore, the variance increase of EOF2 (35%) is larger than that of EOF1 (32%). Dividing the number of months with extreme combined EOF1-EOF2 positive anomalies (Fig. 4B) by the typical 6-month duration of prolonged low sea levels observed around Samoa (*8*), the average frequency of *Taimasa* events increases from about once every 33 years (63 events in 2090 model-years) in the 20th-century CMIP5 experiments to one event every 14 years (146 events in 2090 model-years) in the 21st century. These results are significant according to a bootstrap resampling test (see Materials and Methods), are further supported by strong intermodel agreement (table S1; increase for 16 of 22 selected models), and signify a likely near-doubling in the future number of prolonged sea level drops in the *Taimasa*-affected regions relative to the rising global mean sea level. Conversely, the change in combined negative EOF1 and EOF2 anomalies also suggests the potential for unprecedented coastal inundations in the same parts of the Pacific (multimodel increase is fivefold, Fig. 4B), although it is difficult to estimate a future return period for such sea level high stands without an observational analog and poor multimodel consensus (table S1; 9 models increase and 2 models either decrease or stay the same, but 11 models simulate no extreme inundations in either period) further cautions the result.

Figure 5 shows the observed sea level probability distribution in four island regions (Guam, Samoa, central Line Islands, and Galápagos) that are located in areas of large observed sea level variability (Fig. 2A) as well

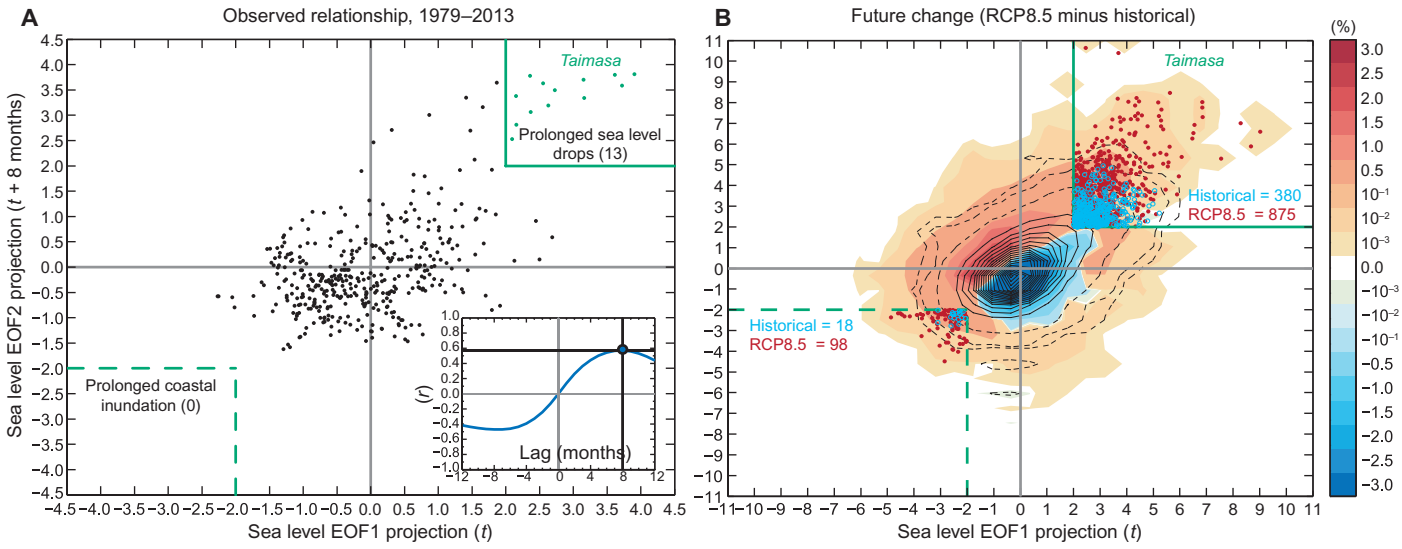

Fig. 4. Observed nonlinear relationship of sea surface height variability and its future change under greenhouse warming. (**A**) Nonlinear and lagged (8-month) relationship between the first and second EOF projection time series of sea surface height anomalies. The inset shows the correlation coefficient between the first and second EOF projections as a function of lag in months (EOF2 lags EOF1 by 8 months, $r = 0.57$). The critical value ($P > 95\%$) for the correlation coefficient is 0.39 based on the autocorrelation decay time scales of the projections. The solid green box encloses the prolonged sea level drops for the tropical southwestern Pacific (*Taimasa*; 13 months observed when both EOF1 and EOF2 projections exceed 2 SDs). Prolonged interannual coastal inundation of similar magnitude and duration has not been observed (dashed green box). (**B**) Projected future change (RCP8.5 minus historical; color scale) and 20th-century (historical; dashed and solid black contours) multimodel probability of occurrence (%) for the principal variability patterns of sea surface height (EOF2 lags EOF1 by 8 months). Contour intervals are nonlinear: 10^{-3}, 10^{-2}, 10^{-1} (dashed), and 1 (solid). A kernel smoothing function (normal distribution; bin width of 1 SD) is applied to the bivariate distribution. An increase in *Taimasa* events (380 versus 875 simulated-months) and prolonged coastal inundation (18 versus 98 simulated-months) from the historical to future period is projected (months when both EOF1 and EOF2 projections exceed ±2 SDs; blue circles, historical; red dots, RCP8.5).

as projected future interannual change exceeding 5% of the historical SD (Fig. 2B). For the historical period, CGCMs generally resolve the observed probability distribution of sea levels in these regions well, although the simulated variance is less than observed (table S2). On interannual time scales in the tropical Pacific, variations of observed and simulated regional sea levels approach the magnitude of global mean sea level rise projections for the middle part of the 21st century (*31*), although extreme sea levels of this size are observed in less than 1% of months.

During the 21st century, the interannual sea level variability is projected to increase in amplitude across most of the tropical Pacific (RCP8.5 minus historical SD > 0) (Fig. 2B and table S2), but the distribution of future changes somewhat varies by region (Fig. 5). In the northwestern Pacific around Guam (Fig. 5A), for example, the change in extreme sea levels is greater for above-average anomalies compared to low sea level events. Such enhanced coastal inundations around Guam would be expected with more negative future extremes of the EOF1 projection (that is, above-normal sea levels in the western Pacific during La Niña); however, likely enhancement of the meridional sea level seesaw would continue to abruptly terminate extreme negative sea level anomalies in the northwestern Pacific (fig. S7), whereas prolonged high sea level stands are projected to increase more in occurrence (fig. S8). For the eastern equatorial Pacific, which is located at the opposite end of the EOF1 zonal sea level seesaw (Fig. 3A, inset), increasing unprecedented sea level drops around the Galápagos Islands (Fig. 5D) during La Niña mirror the projected inundations for Guam, although future coastal inundations are also likely to become more frequent with increasing extreme El Niño events. Because the eastern Pacific is not affected much by the lagged meridional seesaw, particularly near the equator and also along the Central and South American coasts (Fig. 3B, inset), the duration of future extreme low sea level anomalies (fig. S7) is likely to be shorter for the Galápagos Islands (2.7 months year^{-1} <−1 SD on average) compared to *Taimasa*-affected regions in the tropical southwestern Pacific and equatorial central Pacific (3.2 months year^{-1} for both regions).

Rather, it is the regions most affected by the meridional sea level seesaw (EOF2), particularly around Samoa in the southwestern Pacific as well as the equatorial central region around Kiritimati (central Line Islands), that face a combined future threat of more frequent sea level drops (Fig. 5, B and C) and the largest changes in very long-duration events (fig. S7). Future wind-driven changes (figs. S5 and S6) in Samoa (Fig. 5B) and Kiritimati (Fig. 5C) are the largest for the sea level drops, consistent with more positive extreme EOF1 patterns and the long-term positive trend of the EOF2 projection time series in sea level (Figs. 3 and 4B). Because sea level EOF2 lags EOF1 by 8 months, such a trend would also prolong low sea level stands in both regions. For example in Samoa, the probability of an entire year having very low sea levels (<−1 SD)—unprecedented in observations and occurring only three times in the historical simulations—is projected to increase to nearly 6% (125 model-years) (fig. S7).

DISCUSSION

More frequent prolonged sea level drops will increase the exposure time of shallow reefs to air at low tide, a known inhibitor of upward

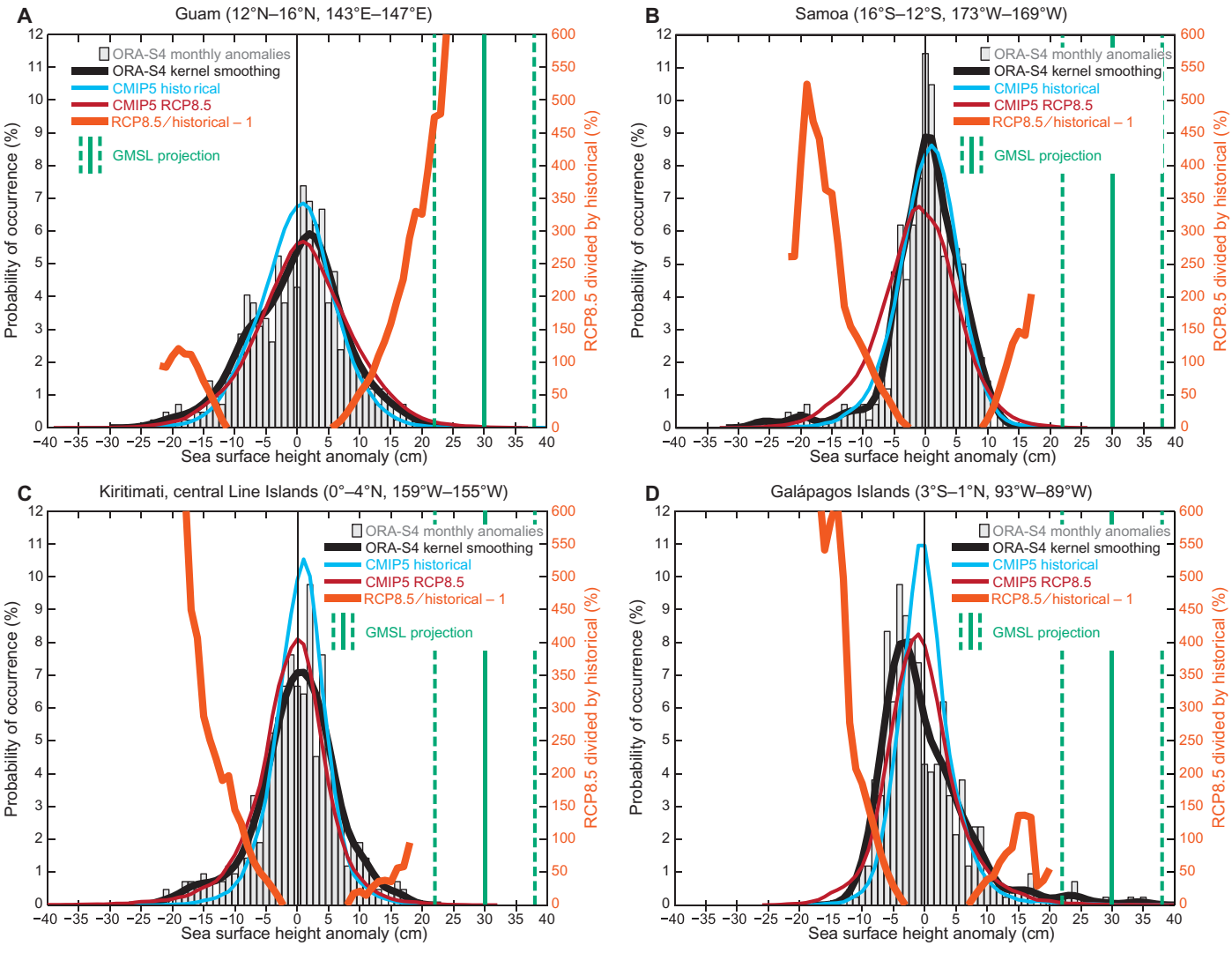

Fig. 5. Probability distribution of observed and simulated sea surface height anomalies (cm) for island regions in the tropical Pacific. (**A** to **D**) Monthly anomalies around Guam, Samoa, Kiritimati in the central Line Islands, and the Galápagos Islands, respectively. Locations are shown in Fig. 2A (4° latitude × 4° longitude averaging regions). A kernel smoothing function (normal distribution; bin width of 1 cm) is applied to each distribution of sea surface heights: black (observations), blue (historical), and red (RCP8.5). The orange line shows the ratio $\frac{\text{RCP8.5}}{\text{historical}} - 1$ (expressed in %) for future values exceeding 0.1% (right axis). For reference, the global mean sea level (GMSL) rise projected for midcentury (2046–2065) is indicated by vertical lines (median and likely range for the RCP8.5 scenario) (*31*).

coral growth (*11*). Considering the multimodel projected future doubling of *Taimasa* events identified here, it seems that this potential sea level stressor on corals should be considered in future assessments of whether coastal reef growth will be able to keep pace with global sea level rise. Conversely to the ecological risks posed by *Taimasa*, prolonged high sea levels—leading to coastal inundations that are so far unprecedented in most parts of the tropical South Pacific including around Samoa—may also become more frequent and intense with greenhouse warming. Regardless of the duration of interannual high sea levels, such anomalies will accelerate the regional risks posed by global sea level rise and any future land subsidence, even as many of these same regions will be faced with an increasing frequency of prolonged extreme sea level drops.

MATERIALS AND METHODS

Experimental design

We use simulated monthly mean sea surface height for the period of 1979–2013 from ORA-S4 (*28*) as a proxy for sea level variability in the observations, thus omitting the effects of vertical land motion such as the ~15-cm sea level rise around Samoa since 2009 (Fig. 1, Pago Pago tide gauge). Monthly anomalies are computed relative to the mean seasonal cycle on the basis of the 35-year climatology. The variability on interannual time scales is highlighted (*8*) here, as opposed to either multidecadal time scales (*32*) or the longer-term sea level rise attributed to greenhouse warming (*33*), by removing any linear trend from the data and also filtering to remove any stochastic noise (frequencies

exceeding 3 months). An extreme sea level event is defined when both the first and second EOF projections exceed ±2 SDs (Fig. 4), corresponding respectively to prolonged sea level drops or potential coastal inundations in the tropical southwestern Pacific. A similar analysis is performed on surface wind stress anomalies (also from ORA-S4) (figs. S4 and S5), and the extreme wind stress–sea surface height relationship is shown in fig. S6. Simulated sea surface height and wind stress anomalies are similarly calculated from CGCMs, except anomalies are with respect to each model's 30-year climatology (1976–2005) and any long-term trends are retained before projecting each model onto the observed EOF patterns.

Following recent studies that found a near-doubling of the future frequency of tropical Pacific climate extremes such as zonal SPCZ events (*18*) and strong El Niño (*23*), we classify 31 CMIP5 CGCMs (*27*) by their ability to simulate these observed nonlinear climate characteristics that have previously been shown to be associated with observed extreme sea level events such as *Taimasa* (*8*). The majority of models (22; table S1) simulate the observed nonlinear relationship between the two leading EOF principal components of the rainfall variability in the tropical Pacific (*18*). One experiment from each model is used, covering the period 1911–2100 using historical anthropogenic and natural forcings to 2005 and then the future emission scenario (RCP8.5), which ignores volcanic and other natural aerosols for the later 95 years. For each model, we first interpolate the dynamic sea surface height and wind stress to the uniform 1° latitude × 1° longitude ORA-S4 grid using bilinear interpolation. We avoid effects of long-term sea level drift by removing each model's global average sea surface height anomaly at each month (fig. S1) but retain the patterns of any long-term sea level trends inherent to the model. (Figure S9 shows the same analysis but with linear trends at every grid point removed from each model.) We derive changes in the frequency of extreme sea level events by comparing the first 95 years (historical period) to the later 95 years (future period); thus, there is a large ratio between the climate change signal and any higher-frequency variability internal to the models.

Statistical analysis

In addition to the two-sample *F* test of the change in multimodel variance of sea level (Fig. 2), we use a bootstrap resampling method to examine whether the change in frequency of extreme sea level drops is statistically significant. The 2090 samples from the 22 selected models in the historical period (95 years) are randomly resampled with replacement to construct 10,000 realizations. The SD of the extreme sea level frequency in the inter-realization is 19 months per 2090 model-years, far smaller than the difference between the historical and the future periods at 495 months per 2090 model-years (Fig. 4B), indicating statistical significance of the difference. The methodology is repeated for prolonged coastal inundation events (inter-realization, 4 months; future change, 80 months), which also shows a significant difference. In the nine models that fail to simulate the observed nonlinear tropical rainfall relationships (table S1), these future sea level changes are not robust (fig. S10).

SUPPLEMENTARY MATERIALS

Supplementary material for this article is available at http://advances.sciencemag.org/cgi/content/full/1/8/e1500560/DC1

Fig. S1. Drift of global average sea surface height anomalies in CMIP5 (zos variable name) for the 20th century (historical) and 21st century (RCP8.5).

Fig. S2. CMIP5 21st-century projections of sea surface height variability on interannual (top) and annual cycle (bottom) time scales for the nine models that do not simulate the observed nonlinear relationship between El Niño and the SPCZ.

Fig. S3. EOF1 and EOF2 patterns of sea surface height variability for the historical (1911–2005) and RCP8.5 (2006–2100) experiments for the 22 models that simulate the observed nonlinear relationship between El Niño and the SPCZ.

Fig. S4. Two principal modes of wind stress variability observed (1979–2013; black lines) in the tropical Pacific and the CMIP5-simulated wind stress anomalies (dots) for the historical (1911–2005) and RCP8.5 (2006–2100) experiments projected onto the observed EOF1 and EOF2 patterns (maps).

Fig. S5. Observed nonlinear relationship of wind stress variability and its future change under greenhouse warming.

Fig. S6. Observed and changing sea surface height projections (*y* axes) as a function of wind stress projections (*x* axes).

Fig. S7. Probability of prolonged interannual sea level drops.

Fig. S8. Probability of prolonged interannual sea level rise.

Fig. S9. Changing sea surface height and wind stress projections with linear trends removed.

Fig. S10. Future change of sea surface height variability under greenhouse warming for the nine models that do not simulate the observed nonlinear relationship between El Niño and the SPCZ.

Table S1. Statistics of CMIP5 models.

Table S2. SDs of observed and simulated sea surface height anomalies (cm) for island regions in the tropical Pacific.

REFERENCES AND NOTES

1. K. Wyrtki, The slope of sea level along the equator during the 1982/1983 El Niño. *J. Geophys. Res.* **89**, 10419–10424 (1984).
2. M. Merrifield, B. Kilonsky, S. Nakahara, Interannual sea level changes in the tropical Pacific associated with ENSO. *Geophys. Res. Lett.* **26**, 3317–3320 (1999).
3. Y.-T. Chang, L. Du, S.-W. Zhang, P.-F. Huang, Sea level variations in the tropical Pacific Ocean during two types of recent El Niño events. *Global Planet. Change* **108**, 119–127 (2013).
4. F.-F. Jin, J. D. Neelin, M. Ghil, El Niño on the Devil's Staircase: Annual subharmonic steps to chaos. *Science* **264**, 70–72 (1994).
5. E. Tziperman, S. E. Zebiak, M. A. Cane, Mechanisms of seasonal–ENSO interaction. *J. Atmos. Sci.* **54**, 61–71 (1997).
6. E. Galanti, E. Tziperman, M. Harrison, A. Rosati, R. Giering, Z. Sirkes, The equatorial thermocline outcropping—A seasonal control on the tropical Pacific Ocean–atmosphere instability strength. *J. Climate* **15**, 2721–2739 (2002).
7. M. F. Stuecker, A. Timmermann, F.-F. Jin, S. McGregor, H.-L. Ren, A combination mode of the annual cycle and the El Niño/Southern Oscillation. *Nat. Geosci.* **6**, 540–544 (2013).
8. M. J. Widlansky, A. Timmermann, S. McGregor, M. F. Stuecker, W. Cai, An interhemispheric tropical sea level seesaw due to El Niño Taimasa. *J. Climate* **27**, 1070–1081 (2014).
9. M. Becker, B. Meyssignac, C. Letetrel, W. Llovel, A. Cazenave, T. Delcroix, Sea level variations at tropical Pacific islands since 1950. *Global Planet. Change* **80–81**, 85–98 (2012).
10. D. Pirhalla, V. Ransi, M. S. Kendall, D. Fenner, in *A Biogeographic Assessment of the Samoan Archipelago*, *NOAA Technical Memorandum NOS NCCOS 132*, M. S. Kendall, M. Poti, Eds. (U.S. Department of Commerce, Silver Spring, MD, 2011), p. 229.
11. C. Woodroffe, R. McLean, Microatolls and recent sea level change on coral atolls. *Nature* **344**, 531–534 (1990).
12. K. Wyrtki, Sea level fluctuations in the Pacific during the 1982–83 El Nino. *Geophys. Res. Lett.* **12**, 125–128 (1985).
13. P. W. Glynn, in *Global Ecological Consequences of the 1982–83 El Niño–Southern Oscillation*, P. W. Glynn, Ed. (Elsevier, Amsterdam, 1990), vol. 52, pp. 55–126.
14. M. R. Chowdhury, P.-S. Chu, T. Schroeder, ENSO and seasonal sea-level variability—A diagnostic discussion for the U.S.-Affiliated Pacific Islands. *Theor. Appl. Climatol.* **88**, 213–224 (2007).
15. F.-F. Jin, An equatorial ocean recharge paradigm for ENSO. Part I: Conceptual model. *J. Atmos. Sci.* **54**, 811–829 (1997).
16. T. Delcroix, Observed surface oceanic and atmospheric variability in the tropical Pacific at seasonal and ENSO timescales: A tentative overview. *J. Geophys. Res.* **103**, 18611–18633 (1998).
17. G. Alory, T. Delcroix, Interannual sea level changes and associated mass transports in the tropical Pacific from TOPEX/Poseidon data and linear model results (1964–1999). *J. Geophys. Res.* **107**, 17-1–17-22 (2002).
18. W. Cai, M. Lengaigne, S. Borlace, M. Collins, T. Cowan, M. J. McPhaden, A. Timmermann, S. Power, J. Brown, C. Menkes, A. Ngari, E. M. Vincent, M. J. Widlansky, More extreme swings of the South Pacific convergence zone due to greenhouse warming. *Nature* **488**, 365–369 (2012).
19. S. McGregor, A. Timmermann, N. Schneider, M. F. Stuecker, M. H. England, The effect of the South Pacific Convergence Zone on the termination of El Niño events and the meridional asymmetry of ENSO. *J. Climate* **25**, 5566–5586 (2012).

20. S. McGregor, N. Ramesh, P. Spence, M. H. England, M. J. McPhaden, A. Santoso, Meridional movement of wind anomalies during ENSO events and their role in event termination. *Geophys. Res. Lett.* **40**, 749–754 (2013).
21. A. Timmermann, S. McGregor, F.-F. Jin, Wind effects on past and future regional sea level trends in the southern Indo-Pacific. *J. Climate* **23**, 4429–4437 (2010).
22. S. McGregor, A. S. Gupta, M. H. England, Constraining wind stress products with sea surface height observations and implications for Pacific Ocean sea level trend attribution. *J. Climate* **25**, 8164–8176 (2012).
23. W. Cai, S. Borlace, M. Lengaigne, P. van Rensch, M. Collins, G. Vecchi, A. Timmermann, A. Santoso, M. J. McPhaden, L. Wu, M. H. England, G. Wang, E. Guilyardi, F.-F. Jin, Increasing frequency of extreme El Niño events due to greenhouse warming. *Nat. Clim. Change* **4**, 111–116 (2014).
24. W. Cai, G. Wang, A. Santoso, M. J. McPhaden, L. Wu, F.-F. Jin, A. Timmermann, M. Collins, G. Vecchi, M. Lengaigne, M. H. England, D. Dommenget, K. Takahashi, E. Guilyardi, Increased frequency of extreme La Niña events under greenhouse warming. *Nat. Clim. Change* **5**, 132–137 (2015).
25. J. Yin, S. M. Griffies, R. J. Stouffer, Spatial variability of sea level rise in twenty-first century projections. *J. Climate* **23**, 4585–4607 (2010).
26. F. W. Landerer, P. J. Gleckler, T. Lee, Evaluation of CMIP5 dynamic sea surface height multi-model simulations against satellite observations. *Clim. Dyn.* **43**, 1271–1283 (2014).
27. K. E. Taylor, R. J. Stouffer, G. A. Meehl, An overview of CMIP5 and the experiment design. *Bull. Am. Meteorol. Soc.* **93**, 485–498 (2012).
28. M. A. Balmaseda, K. Mogensen, A. T. Weaver, Evaluation of the ECMWF ocean reanalysis system ORAS4. *Q. J. R. Meteorol. Soc.* **139**, 1132–1161 (2013).
29. J. G. Dwyer, M. Biasutti, A. H. Sobel, The effect of greenhouse gas–induced changes in SST on the annual cycle of zonal mean tropical precipitation. *J. Climate* **27**, 4544–4565 (2014).
30. S.-P. Xie, C. Deser, G. A. Vecchi, J. Ma, H. Teng, A. T. Wittenberg, Global warming pattern formation: Sea surface temperature and rainfall. *J. Climate* **23**, 966–986 (2010).
31. J. A. Church, P. U. Clark, A. Cazenave, J. M. Gregory, S. Jevrejeva, A. Levermann, M. A. Merrifield, G. A. Milne, R. S. Nerem, P. D. Nunn, A. J. Payne, W. T. Pfeffer, D. Stammer, A. S. Unnikrishnan, Sea level change, in *Climate Change 2013: The Physical Science Basis. Contribution of Working Group I to the Fifth Assessment Report of the Intergovernmental Panel on Climate Change*, T. F. Stocker, D. Qin, G.-K. Plattner, M. Tignor, S. K. Allen, J. Boschung, A. Nauels, Y. Xia, V. Bex, P. M. Midgley, Eds. (Cambridge Univ. Press, Cambridge, 2013).
32. M. A. Merrifield, P. R. Thompson, M. Lander, Multidecadal sea level anomalies and trends in the western tropical Pacific. *Geophys. Res. Lett.* **39**, L13602 (2012).
33. M. A. Merrifield, M. E. Maltrud, Regional sea level trends due to a Pacific trade wind intensification. *Geophys. Res. Lett.* **38**, L21605 (2011).

Acknowledgments: We acknowledge the World Climate Research Programme's Working Group on Coupled Modeling, which is responsible for CMIP, and we thank the climate modeling groups for producing and making available their model output. **Funding:** This work was supported by NSF grant 1049219. **Author contributions:** The paper was written by M.J.W. and A.T. All authors contributed to interpreting the results, improving the methodology, and refining the paper. **Competing interests:** The authors declare that they have no competing interests. **Data and materials availability:** All data are archived at the Asia-Pacific Data-Research Center at the University of Hawai'i at Mānoa (http://apdrc.soest.hawaii.edu).

Submitted 4 May 2015
Accepted 12 June 2015
Published 25 September 2015
10.1126/sciadv.1500560

Citation: M. J. Widlansky, A. Timmermann, W. Cai, Future extreme sea level seesaws in the tropical Pacific. *Sci. Adv.* **1**, e1500560 (2015).